

---

# Instruction Tuning Changes How Upstream State Conditions Late Readout: A Cross-Patching Diagnostic

---

**Yifan Zhou**

University of California, Los Angeles

yifanz1207@gmail.com

Code: [github.com/yifan1207/first-divergence-crosspatching](https://github.com/yifan1207/first-divergence-crosspatching)

Artifact release: `paper-artifacts-v1`

Raw mirror: [gs://pt-vs-it-results/papers/first\\_divergence\\_crosspatching/](https://pt-vs-it-results/papers/first_divergence_crosspatching/)

## Abstract

Recent interpretability work has identified model-internal handles on post-trained behavior, including refusal directions, assistant/persona axes, and sparse chat-tuning features. These results localize where behaviors can be read out or controlled, often in middle-to-late layers. We ask how earlier computation and the late stack cooperate to turn those differences into next-token margins. To test this, we introduce first-divergence cross-patching: at the first token where pretrained base (PT) and instruction-tuned (IT) checkpoints disagree, we cross each model’s earlier-layer state with each model’s late stack. The diagnostic separates training recipes: same-base instruction-following descendants show late effects that depend on their own earlier-layer state, while OpenMath2 math-domain SFT and controlled code/biomed CPT controls with verified domain learning do not; for OpenMath2, the late effect is already largely portable from base earlier-layer state. Across five dense families (4B-32B), the IT late stack adds +0.76 logits from PT upstream and +2.44 from IT upstream, giving a +1.68 interaction that is positive in every family. Thus the late stack has a real PT-upstream effect, but its larger effect in the IT checkpoint appears only when it reads its own post-trained upstream state. Sparse features in final MLP layers partially mediate the effect and are driven by upstream patches, supporting a handoff from earlier state to final-layer feature activation to IT-token margin. Forced-token scoring shows that the local token choice can change later exact-answer success. Operationally, paired-checkpoint studies that localize a difference to late layers should test whether it survives under the other checkpoint’s upstream state before treating the late stack as self-contained.

## 1 Introduction

Where in the forward pass does instruction tuning become a logit? Recent mechanistic interpretability work has found directions, features, and layers that affect post-trained behavior: refusal and harmfulness directions (Arditi et al., 2024; Zhao et al., 2025), assistant/persona axes (Lu et al., 2026), instruction-following steering vectors (Turner et al., 2023; Stolfo et al., 2025), preference-sensitive layers (Du et al., 2025; Chaudhury, 2025), and sparse chat-tuning features (Lindsey et al., 2024; Minder et al., 2025). Many appear in middle-to-late or late layers, where post-training differences are expressed near readout. Our question is how the effect gets there: does post-training mainly change late features themselves, or also the earlier residual states that make those features active? A late-layer feature may affect output only when earlier layers supply the residual pattern it reads.

We measure this coupling with **first-divergence cross-patching**. For each prompt, we find the earliest generated position where PT and IT prefer different next tokens under the same generated history. At that prefix, we pair one checkpoint’s upstream residual state (U\_PT or U\_IT) with one checkpoint’s downstream late stack (L\_PT or L\_IT) and score  $\text{logit}(t_{IT}) - \text{logit}(t_{PT})$ . The difference-in-differences asks how much larger the IT-minus-PT late-stack replacement effect is when the upstream state comes from IT rather than PT, separating the part that transfers to PT upstream from the extra part that requires IT upstream.

At the first PT/IT disagreement, the IT late stack adds +0.76 logits from PT upstream and +2.44 from IT upstream. This is the central story: base-to-instruct differences are not just late-layer features and not just upstream state. The late stack has a real direct effect, but the larger effect appears when upstream computation produces the residual state that activates those late features.

**Result in one place.** Across five dense families (4B-32B), at the first token where PT and IT disagree:

- Late stack from PT upstream: +0.76 logits toward the IT token.
- Late stack from IT upstream: +2.44 logits toward the IT token.
- Interaction: +1.68 logits, positive in 5/5 Core-5 families.
- Training-recipe separation: same-base instruction-following descendants show late effects that depend on their own upstream state; OpenMath2’s math-domain effect is already largely portable from base upstream state (interaction -0.154 on math support), and controlled code/biomed continuation-pretraining controls are near zero on the main support (interactions -0.002, +0.018) despite verified domain learning.
- Effect split: a direct late-stack component plus a larger upstream-dependent component.
- Direct component share: 31.1% family-balanced; family range 19.5-44.3%.

This makes the same four-cell test a worked example of model diffing, not just a measurement of one base/instruct gap. On the same base and architecture, instruction-following descendants require their own upstream state for their late effects; OpenMath2’s math-domain effect is already largely portable from base upstream state, and controlled continuation-trained models do not reproduce the main-support pathway.

**Operational takeaway.** When a paired-checkpoint study localizes a difference to late layers, report the same late-stack effect under both its own checkpoint’s upstream state and the other checkpoint’s upstream state. A late effect measured only in its own checkpoint shows where the effect appears; by itself it does not show that the computation is self-contained.

**Behavioral scope.** The main claim is local: it concerns the first moment where released base and instruct checkpoints choose different next tokens. Forced-token scoring improves suffix-only exact-answer success on CONTENT-REASON prompts, and constrained continuation shows short-horizon persistence, but broad free-running behavior is not the load-bearing claim.

The paper has three contributions.

1. **A cross-patching diagnostic for upstream dependence.** First-divergence cross-patching decomposes the IT-minus-PT late-stack replacement effect into PT-upstream and IT-upstream components.
2. **Training-recipe separation across same-base descendants.** This is the main empirical payoff: instruction-following descendants show late effects that depend on their own upstream state, while OpenMath2 and controlled continuation-pretraining controls show that this pattern is not automatic same-base post-training.
3. **Mechanistic and downstream checks.** Crosscoders on final MLP layers identify sparse features that partially mediate, gate, and rescue the interaction; forced-token scoring and constrained continuation show later exact-answer consequences and short-horizon persistence. These are supporting checks, not full circuit reconstruction or broad behavior estimates.

Scope is intentionally local. In Core-5 contrasts, **PT** is the released pretrained/base checkpoint and **IT** is the released instruction-following descendant; recipe and lineage checks name stages explicitly.

## 2 Setup

### 2.1 Model Sets and Statistical Reporting

The main factorial uses five dense PT/IT pairs: Llama 3.1 8B, Qwen 3 4B, Mistral 7B, OLMo 2 7B, and Qwen2.5 32B. Appendix A gives revisions, prompt supports, valid-event counts, position mix, and late-stack boundaries.

Prompt-bootstrap intervals quantify precision on the sampled prompts and released checkpoints, not over all model families, recipes, or prompt distributions. We therefore report Core-5 means plus family ranges or medians where useful. The Appendix Roadmap maps claims to audit trails and artifact roots.

### 2.2 First-Divergence Cross-Patching Factorial

Starting from the raw prompt, we compare PT and IT greedy top-1 predictions step by step. Until the first disagreement, the generated prefix is identical by construction; the first position where their top-1 next tokens differ defines the intervention site. Let those tokens be  $t_{PT}$  and  $t_{IT}$ , and define  $Y(U,L) = \text{logit}(t_{IT}) - \text{logit}(t_{PT})$ .

Larger  $Y$  means the hybrid forward pass favors the IT divergent token. Late-stack boundaries were fixed before Core-5 synthesis using a consistent architecture-relative rule: the late stack starts at roughly 60% depth and includes the final blocks. Appendix A gives full per-family boundaries. We then run the four cells below:

**Table 1: Four-cell cross-patching factorial.**

Upstream state	PT late stack $L_{PT}$	IT late stack $L_{IT}$
PT upstream $U_{PT}$	$Y(U_{PT},L_{PT})$	$Y(U_{PT},L_{IT})$
IT upstream $U_{IT}$	$Y(U_{IT},L_{PT})$	$Y(U_{IT},L_{IT})$

Conceptually, the primary quantity is the interaction effect of instruction tuning on the late-stack replacement: how much more the IT late stack helps when it reads IT upstream state rather than PT upstream state. Formally:

$$[Y(U_{IT},L_{IT}) - Y(U_{IT},L_{PT})] - [Y(U_{PT},L_{IT}) - Y(U_{PT},L_{PT})].$$

Equivalently: measure the IT-minus-PT late-stack replacement effect under each upstream state, then compare those two effects. Common-IT and common-PT readouts score all cells with one fixed final norm, `lm_head`, and real-token mask; main numbers use common-IT readout unless stated otherwise.

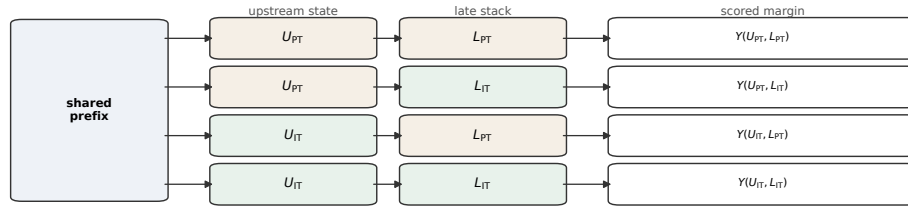
**What this quantity measures.** First-divergence cross-patching is a local next-token readout test. It does not estimate average instruction-following behavior or claim that hybrid states are natural trajectories. It tests how the IT late-stack replacement effect changes between PT and IT upstream residual states at natural PT/IT disagreement prefixes.

**Hybrid forward-pass implementation.** Cached decoding is used only to find the shared prefix. Each scored cell is recomputed as a full `use_cache=False` forward pass over the raw prompt plus shared generated prefix. The patch replaces the full hidden-state tensor entering the late-boundary layer, so the downstream late stack recomputes attention keys and values for all prefix positions. The unmodified PT/PT and IT/IT cells are runtime-checked against the original forward pass.

All raw-shared runs force PT and IT branches to raw text and validate identical prompt token IDs before residual comparisons. This alignment is necessary for position-wise patching, but evaluates IT checkpoints without native chat templates; we interpret the result as a raw-shared upstream-dependence test, not a native-chat behavior estimate.

### A. Four hybrid passes at the first divergence

Same raw prompt and generated prefix. Readout:  $Y = \text{logit}(t_{IT}) - \text{logit}(t_{PT})$ .



$$\text{interaction} = [Y(U_{IT}, L_{IT}) - Y(U_{IT}, L_{PT})] - [Y(U_{PT}, L_{IT}) - Y(U_{PT}, L_{PT})]$$

Interpretation: how much more the IT late stack helps when it reads an IT-shaped upstream state.

### B. Concrete divergent-token examples

Model	Prompt fragment	pos.	PT token	IT token
Mistral 7B	Question: What is the difference between a podcast and...	4	'radio'	'digital'
OLMo 2 7B	Question: What causes the seasons? Answer:	3	'axis'	'tilt'
Qwen 3 4B	Write a startup pitch for a time capsule service. The...	5	'1'	'3'
Llama 3.1 8B	Question: My landlord is refusing to fix the heating...	13	'legal'	'several'

Examples are illustrative; all statistics use the full first-divergence support.

Figure 1: First-divergence schematic and token examples. Panel A shows the four hybrid passes used to estimate the upstream x late interaction. Panel B gives illustrative divergent-token pairs; all quantitative claims use the full support in Appendix A.

## 3 Results

### 3.1 Main Upstream-Late Decomposition

The four-cell result separates three interpretations of a late-stack effect: self-contained across upstream states, not useful under PT upstream, or dependent on IT upstream state. Replacing the PT late stack with the IT late stack shifts the IT-token margin by +0.76 logits from PT upstream, but by +2.44 logits from IT upstream. The headline magnitude is the +1.68 interaction: a direct late-stack component is present, but most of the effect seen in the IT checkpoint appears only with IT upstream state.

The verdict is simple. A self-contained account is disfavored because the effect in the IT checkpoint is much larger than the PT-upstream effect. A no-transfer account is also disfavored because the PT-upstream component is +0.76 logits. The supported picture is upstream-late coupling.

The sign pattern is consistent across families: every Core-5 interaction is positive, ranging from +1.25 to +2.53 logits. The direct late-stack share ranges from 19.5% to 44.3% across families, with median 29.2% and family-balanced center 31.1%. We treat the logit interaction as primary; Appendix B reports scale conversions.

The interaction is also not confined to response openings: generated position  $\geq 3$  and  $\geq 5$  subsets remain positive, though smaller and thinner.

**Table 2: Core-5 headline four-cell effects.**

Scope	PT-up late	IT-up late	Interaction
Core-5, common-IT	+0.76	+2.44	+1.68
Core-5, common-PT	+0.78	+2.49	+1.70
Qwen2.5-32B only	+1.04	+2.34	+1.30

The +1.68 interaction multiplies the odds of  $t_{IT}$  over  $t_{PT}$  by about 5.4x within the constructed contrast. This is still local token-margin evidence, not a deployment behavior estimate. On a

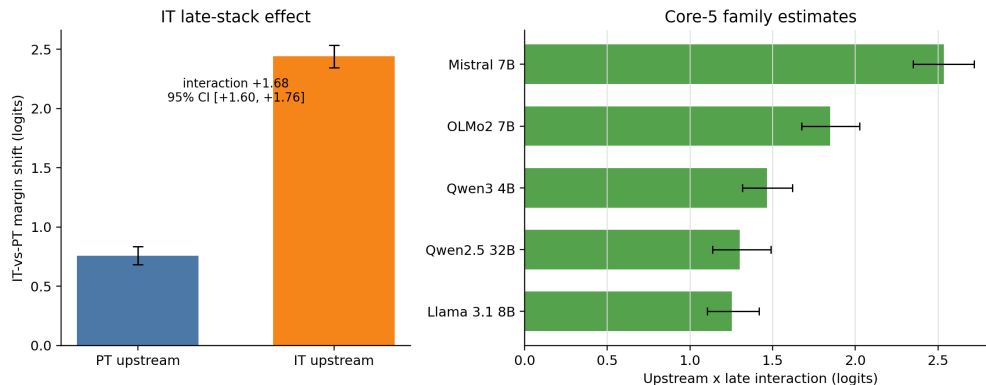


Figure 2: Core-5 first-divergence interaction by family. The upstream x late interaction is positive in every core dense family, including Qwen2.5 32B.

factual/reasoning-enriched stress support, the PT-upstream late effect is negative (-1.18) while the interaction remains positive (+1.81).

### 3.2 Training-Recipe Separation: Same Base, Different Dependence on Earlier Layers

The same four-cell test separates instruction-following descendants from same-base domain and task controls. This is the clearest example of why the foreign-upstream cell matters: two descendants of the same base can both have strong late effects in their own checkpoint, but for different reasons. OpenMath2 shares the Llama-3.1-8B base and architecture with the instruction descendants (Toshniwal et al., 2024). On math prompts, its late stack has a large effect, and that effect still appears when it reads the base model’s earlier-layer state. Instruction-following descendants behave differently: their late effects are much stronger when they read their own earlier-layer state.

**Recipe summary.** OpenMath2 is not a no-effect control: on math prompts, its late effect is large but portable (interaction -0.154; PT-up +3.430; own-up +3.275). Instruction descendants are upstream-dependent on both instruction prompts (+0.959) and math prompts (+1.670), giving an instruction-minus-OpenMath2 matched contrast of +1.335. Controlled code and biomedical CPT adapters improve held-out domain NLL and pass merge/generation-health checks, but do not reproduce the instruction-prompt pattern on the main support (-0.002 / +0.018); biomedical CPT shows a domain-local interaction on biomedical prompts (+0.283).

Appendix F gives per-descendant recipe controls and the fixed-support lineage tables.

Consequence and persistence checks support the interpretation without replacing the token-level measurement. They are not benchmark claims: they ask whether the local token choice can matter downstream under controlled continuations. On CONTENT-REASON exact-answer prompts, forcing the descendant-preferred divergent token improves suffix-only objective success by +0.157 [+0.120,+0.192]; the forced token itself is excluded from scoring. Constrained continuation stays positive through N=8, coherent descendant tails carry more interaction than shuffled tails, and OpenMath2 again behaves differently.

Appendix F also gives fixed-support lineage checks for released Tulu-3 and OLMo-2 post-training sequences (Lambert et al., 2025; Team OLMo et al., 2025): we score SFT, DPO, and Final/RLVR checkpoints on the same Base-to-Final first-divergence support. SFT is nonzero and DPO/preference checkpoints are near final; these cumulative comparisons show coherence across lineages, not causal stage attribution.

### 3.3 Validation Against Hybrid and Selection Artifacts

First divergence is not chosen as a representative average over all tokens. It is chosen because it is the first position where the paired checkpoints define a meaningful next-token contrast: PT prefers  $t_{PT}$ , IT prefers  $t_{IT}$ , and the margin  $Y = \text{logit}(t_{IT}) - \text{logit}(t_{PT})$  asks how that preference is formed.

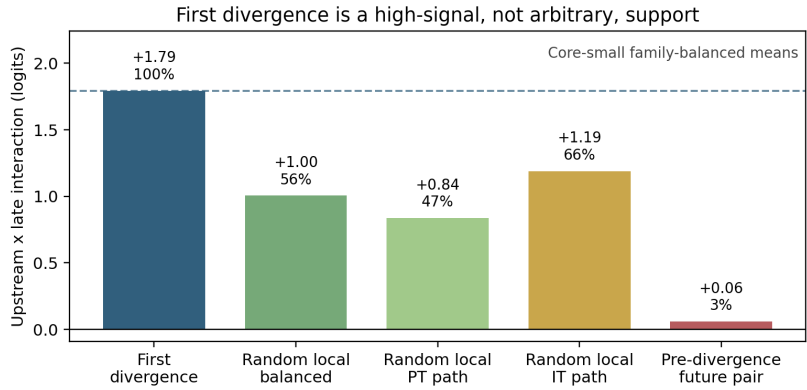


Figure 3: Selection baselines for first divergence. Random local disagreements from the same rollouts preserve the sign of the upstream x late interaction at reduced magnitude, while pre-divergence future-token scoring is near zero. Values are Core-small family-balanced means.

Measuring every token would mostly mix in positions where the checkpoints agree and no PT-vs-IT label contrast is available.

The validation question is therefore narrower than naturalness: after conditioning on a real PT/IT next-token decision, what would make the four-cell test uninformative? We focus on three failure modes. The hybrid state could be broken; the first-disagreement support could be an arbitrary selection artifact; or the token could already be decided before the late stack, so the late-stack interaction is only a readout convention.

The strongest selection check is shown in Figure 3. Random later PT/IT disagreements from the same rollouts preserve the sign at reduced magnitude (56%), while scoring the future divergent token pair before the models diverge is near zero (3%). This means first divergence concentrates the effect, but it is not a magic position: related local disagreements retain a weaker version, and prefixes before the disagreement do not.

The other main checks address implementation and scope. Hybrid-state diagnostics make implementation failure and gross off-manifold collapse unlikely: unmodified diagonal cells reconstruct exactly, PT-to-IT boundary interpolation is smooth and positive, and matched signed-permutation patches recover only 0.31x of the endpoint effect. Native-history local disagreements drop the exact shared-history requirement and remain positive after greedy IT histories (+1.51 logits [+1.42,+1.61]) and in the PT-history mirror (+1.49 [+1.33,+1.65]), with all four Core-small dense families positive in both directions. Pre-late commitment controls still find a positive interaction when the IT boundary readout does not yet favor  $t_{IT}$ .

The readout-swap agreement, label-swap null, later-position subsets, and full selected-support audit are kept in Appendix C. Taken together, the controls do not prove that hybrid trajectories are natural deployment trajectories, nor do they turn a token-level diagnostic into an average behavior estimate. They show that the upstream-dependent late-stack pattern survives the artifact tests that would make the factorial uninformative.

### 3.4 Mechanistic Evidence: Sparse Final-Layer Features and Structured State

These analyses ask whether part of the interaction can be traced to sparse MLP features near the end of the network and to structured residual-state shifts. The proposed path is earlier-layer computation -> final-layer sparse features -> IT-token margin. Window anatomy motivates focusing on final MLP layers; the feature analysis is partial evidence, and boundary-state closure is an independent residual-state check. This is not full circuit reconstruction.

We use two units in this section. **Feature rescue** means an absolute logit gain in the weak  $U_{PT,L_{IT}}$  hybrid. The **missing margin** is the gap between native IT-upstream readout and the weak hybrid,  $Y(U_{IT,L_{IT}}) - Y(U_{PT,L_{IT}})$ ; closure fractions divide a gain by this missing margin.

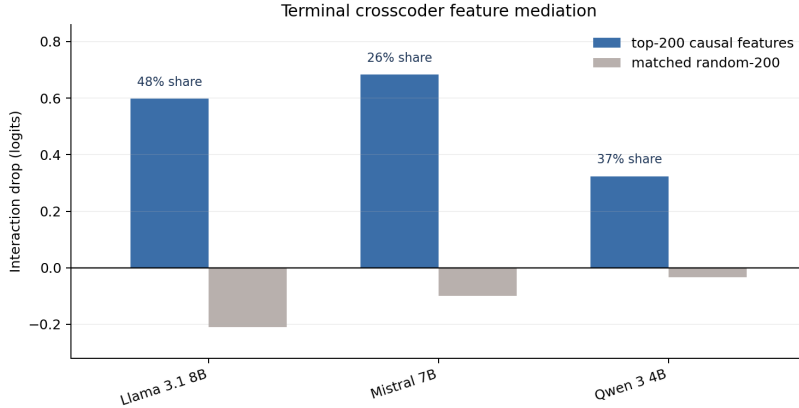


Figure 4: Final-layer crosscoder mediation. Ablating the top causally ranked final-layer features reduces the upstream  $\times$  late interaction in each quality-gated final-layer-crosscoder family, while matched random features do not reproduce the effect. Percent labels show the top-200 share of the family interaction.

### 3.4.1 Window Anatomy

The window-level anatomy shows a candidate-to-margin pattern: middle windows transfer divergent-token identity more often, while late and terminal windows are more margin-sensitive. Middle-positioned MLP substitutions transfer which token wins more often than late substitutions, while late windows dominate IT-token support under IT upstream state. Terminal-depth audits in Appendix D sharpen the same story. This is an operational depth pattern rather than a complete circuit.

### 3.4.2 Sparse Final-Layer Features Carry a Concentrated Part

Crosscoders on final MLP outputs connect the window-level pattern to sparse features in the three families that pass the predeclared crosscoder quality gate. We train paired PT/IT BatchTopK crosscoders (Lindsey et al., 2024; Minder et al., 2025) on final MLP outputs, rank features by held-out causal effect, and ablate their IT-branch decoder contribution inside the IT final layers. The fixed top-200 subset accounts for 26-48% of the final-layer readout interaction in these quality-gated families, while matched-random sets have the wrong sign or near-zero effect.

For the feature edits below, rescue is an absolute logit gain; rescue fractions in Appendix E divide by the missing margin defined above.

### 3.4.3 Upstream Patches Drive Final-Layer Features

Within the same quality-gated families, the sparse final-layer features inherit the upstream dependence seen at window level. Ablating the top-200 causal final-layer features hurts the  $U_{IT}, L_{IT}$  readout much more than the  $U_{PT}, L_{IT}$  readout, and patching their activations from the  $U_{IT}, L_{IT}$  pass into the weak  $U_{PT}, L_{IT}$  hybrid gives a +0.49 logit rescue. Both effects beat matched-random controls. This is not full reconstruction, but it recovers a measurable slice of the missing IT-token margin.

A direct upstream-patch test perturbs earlier computation and re-measures the same final-layer features. Injecting IT middle-to-late computation before the final layers into the weak  $U_{PT}, L_{IT}$  hybrid rescues +1.71 logits, with +0.13 mediated by selected final-layer features. The reverse PT patch into the  $U_{IT}, L_{IT}$  pass causes a +3.57 drop, with +0.53 mediated. Thus earlier-state changes drive a measurable part of final-layer sparse-feature readout.

### 3.4.4 Independent Structured Boundary-State Closure

This is an independent state-space check, not a crosscoder result. On Llama-3.1 descendants, we fit PCA directions to train-split descendant-minus-base boundary-state shifts and inject held-out projections into the weak base-upstream/descendant-late hybrid. At terminal boundary 31, a rank-256 projection closes 0.71 of the missing IT-token margin; the full held-out delta gives the expected upper

bound (0.97). Matched Gaussian and random full directions are near zero, and sign-flipped directions go negative. We use this as structured residual-state support, not as a recipe-level or completion-level claim.

## 4 Related Work

**Late refinement and post-training diffs.** Feed-forward layers promote vocabulary-space concepts and refine predictions (Geva et al., 2021, 2022), and layerwise/tuned-lens or layer-contrast analyses describe late residual sharpening and confidence adjustment (nostalgebraist, 2020; Belrose et al., 2023; Chuang et al., 2024; Lad et al., 2025; Joshi et al., 2025). Fine-tuning and post-training studies report low-dimensional, localized, or layerwise shifts in trained models (Aghajanyan et al., 2021; Panigrahi et al., 2023; Lin et al., 2024; Wu et al., 2024; Zhao, Ziser, and Cohen, 2024; Du et al., 2025; Chaudhury, 2025). Instruction Vectors find complementary early-to-late conditionality (Bigoulaeva et al., 2026), while Sparse but Critical analyzes reinforcement-learning-with-verifiable-rewards (RLVR) token substitutions during sampling (Meng et al., 2026). Divergent-token metrics also use token-level changes as degradation signals (Deiseroth et al., 2024); our question is internal to paired checkpoints at the selected disagreement token.

**Activation patching, steering axes, and sparse model diffs.** Activation patching requires care because metric choice, intervention direction, and off-manifold hybrids affect interpretation (Heimersheim and Nanda, 2024). Representation-engineering and activation-steering work identifies directions and layers associated with sentiment, refusal, harmfulness, assistant persona, and instruction following (Zou et al., 2023; Turner et al., 2023; Rimsky et al., 2024; Arditì et al., 2024; Stolfo et al., 2025; Zhao et al., 2025; Lu et al., 2026). Our contribution is to make upstream dependence of a localized late effect measurable by scoring the same late-stack replacement under its own checkpoint’s upstream state and the other checkpoint’s upstream state. Cross-model activation patching is the closest methodological precedent (Prakash et al., 2024), but asks whether fine-tuning enhances an existing task circuit; ours asks how the IT late-stack replacement depends on upstream state at a natural PT/IT disagreement. Unlike global sparse model-diff work (Lindsey et al., 2024; Minder et al., 2025), and complementary to sparse-autoencoder evaluation work (Makelov et al., 2024), we apply crosscoders after defining the causal quantity and ask which final-layer features mediate it. Full circuit discovery is a separate goal (Conmy et al., 2023).

**Novelty.** Prior work localizes fine-tuning effects, steering directions, or chat-specific features; here upstream-late coupling is the measured object. We score the same late-stack replacement under PT and IT upstream states at a natural PT/IT disagreement, decomposing one late-stack effect into a direct part and an upstream-dependent part. Instruction Vectors give convergent qualitative evidence; our contribution is the paired-checkpoint causal decomposition and sparse-feature evidence for the PT/IT readout margin.

## 5 Discussion, Scope, and Next Tests

### 5.1 Interpretation

Released base-to-instruct contrasts appear to reshape how upstream computation prepares late readout, not merely change a standalone late stack. Our evidence is scoped to dense checkpoint pairs, first-divergence token readouts, and constructed cross-patches.

The same-base recipe check sharpens the interpretation: OpenMath2 has a large math-domain late effect that is already largely portable from base upstream state, while instruction-following descendants depend more on their own upstream state. Tulu-3 and OLMo-2 show the quantity can be reused along released lineages, but these are cumulative checkpoint comparisons, not stage attributions.

A plausible reason is that instruction following is a many-context control problem rather than a single domain skill. It mixes task framing, output format, refusal/helpfulness style, and candidate selection, so late features may only become useful after earlier layers encode which mode the prompt calls for. OpenMath2 may instead make pretrained math machinery easier to elicit: the base upstream state already carries enough of the relevant computation, and the fine-tune mainly improves how late

layers read it out. The CPT controls show domain-local coupling can arise without reproducing the instruction-prompt pathway. We treat this as interpretation, not a full circuit explanation.

The behavioral connection is deliberately narrower than a benchmark claim. Local token margins are the right unit for this diagnostic because the intervention is a next-token counterfactual. Forced-token scoring improves later suffix-only exact-answer success on CONTENT-REASON prompts, and constrained continuation shows fixed-continuation persistence.

## 5.2 Scope

The primary measurement is local to first-divergence next-token readouts; native-history checks show a same-sign local-disagreement variant, but neither is an average over deployment behavior. The interventions are window-level compatibility tests: validation makes practical hybrid artifacts unlikely, constrained continuation shows short-horizon likelihood persistence, and crosscoders expose a partial, quality-gated sparse-feature trace near the final MLP layers. The raw-shared design is intentional because exact residual comparisons require aligned token IDs.

The empirical scope is five dense core PT/IT pairs including one 32B pair, same-base released and controlled recipe controls, and two released dense lineages. DeepSeek-V2-Lite is artifact-only because MoE routing and expert swaps need different controls; architecture and MoE generalization remain next-step questions.

## 5.3 Practical Implications and Next Tests

For paired checkpoints, a large late effect measured only in its own checkpoint shows where the effect appears but does not show whether the computation is self-contained or depends on upstream state. The four-cell test distinguishes direct late-stack contribution, upstream-dependent contribution, and no useful late-stack transfer; next work should identify middle-to-late drivers of the final-layer features.

## 6 Conclusion

First-divergence cross-patching turns “do late layers explain the base-to-instruct difference?” into an upstream-late coupling test. At the first PT/IT disagreement, the IT-minus-PT late-stack replacement effect decomposes into a positive direct component from PT upstream and a larger component that appears with IT upstream state. The result is positive across five dense families, separates training recipes under released and controlled same-base comparisons, is coherent along two lineages, and is robust to artifact and native-history checks.

Taken together, the results support an upstream-to-late cooperation story rather than a standalone late-stack story: released base-to-instruct contrasts show upstream-state differences that condition late readout, and the same four-cell test reveals both this coupling and training-recipe differences.

## References

- Aghajanyan, A., Gupta, S., & Zettlemoyer, L. (2021). Intrinsic Dimensionality Explains the Effectiveness of Language Model Fine-Tuning. *ACL-IJCNLP 2021*.
- Arditi, A., et al. (2024). Refusal in Language Models Is Mediated by a Single Direction. *NeurIPS 2024*. arXiv:2406.11717.
- Belrose, N., et al. (2023). Eliciting Latent Predictions from Transformers with the Tuned Lens. arXiv:2303.08112.
- Bigoulaeva, I., Rohweder, J., Dutta, S., & Gurevych, I. (2026). Patches of Nonlinearity: Instruction Vectors in Large Language Models. arXiv:2602.07930.
- Bills, S., et al. (2023). Language Models Can Explain Neurons in Language Models. OpenAI. <https://openai.com/index/language-models-can-explain-neurons-in-language-models/>.
- Chuang, Y., et al. (2024). DoLa: Decoding by Contrasting Layers Improves Factuality in Large Language Models. *ICLR 2024*.
- Chaudhury, A. (2025). Alignment is Localized: A Causal Probe into Preference Layers. arXiv:2510.16167.
- Cobbe, K., et al. (2021). Training Verifiers to Solve Math Word Problems. arXiv:2110.14168.
- Conmy, A., et al. (2023). Towards Automated Circuit Discovery for Mechanistic Interpretability. *NeurIPS 2023*.
- Deiseroth, B., et al. (2024). Divergent Token Metrics: Measuring Degradation to Prune Away LLM Components – and Optimize Quantization. *NAACL 2024*.
- Du, H., et al. (2025). How Post-Training Reshapes LLMs: A Mechanistic View on Knowledge, Truthfulness, Refusal, and Confidence. *COLM 2025*. arXiv:2504.02904.
- Geva, M., Schuster, R., Berant, J., & Levy, O. (2021). Transformer Feed-Forward Layers Are Key-Value Memories. *EMNLP 2021*.
- Geva, M., et al. (2022). Transformer Feed-Forward Layers Build Predictions by Promoting Concepts in the Vocabulary Space. *EMNLP 2022*.
- Heimersheim, S., & Nanda, N. (2024). How to Use and Interpret Activation Patching. arXiv:2404.15255.
- Hendrycks, D., et al. (2021). Measuring Massive Multitask Language Understanding. *ICLR 2021*. arXiv:2009.03300.
- Hu, E. J., et al. (2022). LoRA: Low-Rank Adaptation of Large Language Models. *ICLR 2022*. arXiv:2106.09685.
- Huang, J., et al. (2023). Rigorously Assessing Natural Language Explanations of Neurons. *Black-boxNLP 2023*.
- Joshi, A., Ahmad, A., & Modi, A. (2025). Calibration Across Layers: Understanding Calibration Evolution in LLMs. *EMNLP 2025*.
- Lad, V., et al. (2025). The Remarkable Robustness of LLMs: Stages of Inference? *NeurIPS 2025*.
- Lambert, N., et al. (2025). Tulu 3: Pushing Frontiers in Open Language Model Post-Training. *COLM 2025*.
- Lin, B. Y., et al. (2024). The Unlocking Spell on Base LLMs: Rethinking Alignment via In-Context Learning. *ICLR 2024*.
- Lindsey, J., et al. (2024). Sparse Crosscoders for Cross-Layer Features and Model Diffing. *Transformer Circuits Thread*. <https://transformer-circuits.pub/2024/crosscoders/>.
- Lu, C., Gallagher, J., Michala, J., Fish, K., & Lindsey, J. (2026). The Assistant Axis: Situating and Stabilizing the Default Persona of Language Models. arXiv:2601.10387.

Makelov, A., Lange, G., & Nanda, N. (2024). Towards Principled Evaluations of Sparse Autoencoders for Interpretability and Control. arXiv:2405.08366.

Meng, H., et al. (2026). Sparse but Critical: A Token-Level Analysis of Distributional Shifts in RLVR Fine-Tuning of LLMs. arXiv:2603.22446.

Minder, J., et al. (2025). Overcoming Sparsity Artifacts in Crosscoders to Interpret Chat-Tuning. *NeurIPS 2025*. arXiv:2504.02922.

nostalgebraist. (2020). Interpreting GPT: The Logit Lens. LessWrong. <https://www.lesswrong.com/posts/AcKRB8wDpdaN6v6ru/interpreting-gpt-the-logit-lens>.

Panigrahi, A., et al. (2023). Task-Specific Skill Localization in Fine-tuned Language Models. *ICML 2023*.

Prakash, N., et al. (2024). Fine-Tuning Enhances Existing Mechanisms: A Case Study on Entity Tracking. *ICLR 2024*.

Rafailov, R., et al. (2023). Direct Preference Optimization: Your Language Model is Secretly a Reward Model. *NeurIPS 2023*. arXiv:2305.18290.

Rimsky, N., Gabrieli, N., Schulz, J., Tong, M., Hubinger, E., & Turner, A. (2024). Steering Llama 2 via Contrastive Activation Addition. *ACL 2024*. arXiv:2312.06681.

Roettger, P., et al. (2024). XSTest: A Test Suite for Identifying Exaggerated Safety Behaviours in Large Language Models. *NAACL 2024*. arXiv:2308.01263.

Stolfo, A., Balachandran, V., Yousefi, S., Horvitz, E., & Nushi, B. (2025). Improving Instruction-Following in Language Models through Activation Steering. *ICLR 2025*. arXiv:2410.12877.

Team OLMo et al. (2025). 2 OLMo 2 Furious (COLM’s Version). *COLM 2025*.

Toshniwal, S., et al. (2024). OpenMathInstruct-2: Accelerating AI for Math with Massive Open-Source Instruction Data. arXiv:2410.01560.

Turner, A. M., et al. (2023). Steering Language Models With Activation Engineering. arXiv:2308.10248.

Wu, X., et al. (2024). From Language Modeling to Instruction Following: Understanding the Behavior Shift in LLMs after Instruction Tuning. *NAACL 2024*.

Zhao, W., et al. (2024). WildChat: 1M ChatGPT Interaction Logs in the Wild. arXiv:2405.01470.

Zhao, J., Huang, J., Wu, Z., Bau, D., & Shi, W. (2025). LLMs Encode Harmfulness and Refusal Separately. arXiv:2507.11878.

Zhao, Z., Ziser, Y., & Cohen, S. B. (2024). Layer by Layer: Uncovering Where Multi-Task Learning Happens in Instruction-Tuned Large Language Models. *EMNLP 2024*.

Zheng, L., et al. (2023). Judging LLM-as-a-Judge with MT-Bench and Chatbot Arena. *NeurIPS 2023 Datasets and Benchmarks*. arXiv:2306.05685.

Zhou, J., et al. (2023). Instruction-Following Evaluation for Large Language Models. arXiv:2311.07911.

Zou, A., Wang, Z., Kolter, J. Z., & Fredrikson, M. (2023). Universal and Transferable Adversarial Attacks on Aligned Language Models. arXiv:2307.15043.

Zou, A., et al. (2023). Representation Engineering: A Top-Down Approach to AI Transparency. arXiv:2310.01405.

## Appendix Roadmap

The main text is written around stable claim names. For details, start with Appendix B for the main four-cell factorial, Appendix F for recipe discrimination, Appendix C for validation controls, and Appendix E for sparse final-layer features. Numeric run IDs appear only in file paths or script names; they are provenance labels, not concepts the reader needs to parse.

**Table R.1: Claim roadmap.**

Claim	Main location	Appendix	Artifact/script pointer
Minimal reproducibility snapshot	Sec. 2.1	A, B, H	model registry, dataset manifests, raw first-divergence records
Core-5 first-divergence interaction and scale conversions	Sec. 3.1	B	Core synthesis artifacts and first-divergence collectors
Training-recipe separation and downstream checks	Sec. 3.2	F	same-base Llama recipe controls including controlled non-instruction CPT controls; forced-token objective check; constrained continuation check; fixed-support Tulu-3 and OLMo-2 Base/SFT/DPO/Final stage sweeps
Validation ladder	Sec. 3.3	C	hybrid-state validation, random-disagreement baselines, native-history local-disagreement check, token-support audit, pre-late logit-commitment control
Depth and final-layer anatomy	Sec. 3.4	D	identity/margin handoff, final-depth audit, final-MLP audit
Final-layer feature mediation, upstream dependence, rescue, structured boundary-state closure, handoff, and structure-bucket validation	Sec. 3.4	E	final-layer crosscoder synthesis, hardening runs, upstream-dependence audit, feature rescue, structured boundary-state closure, earlier-to-final-layer handoff, autointerp taxonomy, structure-readout edit
Architecture and MoE scope	Sec. 5	G	dense/MoE scope note

Prompt-bootstrap CIs in the main text are conditional precision estimates over sampled prompts and released checkpoints. They are paired with family-level summaries or family ranges where a claim could otherwise be mistaken for a population-level model-family generalization.

**Table R.2: What each appendix supports.**

Appendix	Supports	Does not prove
A	Model scope, prompt supports, sampling, revision pins, boundary choices, and dataset documentation.	Population-level model-family generalization or template-aware deployment behavior.
B	Core-5 interaction magnitude, secondary scale conversions, family consistency, and readout robustness.	Population-level generalization over all dense or post-trained models.
C	Main artifact explanations are unlikely: broken hybrids, arbitrary token support, first-divergence-only support, and pre-late logit commitment.	Hybrid passes are natural deployment trajectories or completion-level behavior estimates.
D	Depth anatomy: middle windows are relatively more identity-selective while late/terminal windows are more margin-sensitive.	A complete circuit or a unique layer boundary.
E	Sparse final-layer features partially mediate, gate, and rescue the final-layer readout interaction; structured boundary-state shifts close much of the missing margin.	Full mechanism recovery, recipe-unique boundary directions, or feature monosemanticity.
F	Same-base released and controlled recipe controls, constrained continuation scoring, forced-token objective scoring, and two released dense lineages show that the result is not an automatic consequence of fine-tuning/CPT, a one-token artifact, or one final checkpoint accident.	Isolated causal attribution to SFT, DPO, or RLVR algorithms, broad completion-level behavioral interaction, or natural-rollout behavior for every recipe.
G	Dense-family scope and MoE limitations are explicit.	MoE generalization.
H	Reviewer-facing reproduction levels and artifact roots.	That full raw GPU reruns are cheap.

## A Model Scope and Statistical Reporting

**Claim supported.** The paper uses fixed released checkpoint pairs, fixed prompt supports, and a consistent statistical reporting convention.

**Primary evidence.** Full checkpoint revisions, prompt mixes, and the exact scale definitions used in Sec. 3.1.

**What this does not prove.** The released checkpoints are not controlled training-recipe ablations.

**Where to audit.** Model registry, dataset manifests, and artifact roots are consolidated in Appendix H.

**Core-5 set.** Llama 3.1 8B, Qwen 3 4B, Mistral 7B, OLMo 2 7B, and Qwen2.5 32B. Qwen2.5 32B is included as the scale check in the core first-divergence synthesis.

**Core-small support set.** Llama 3.1 8B, Qwen 3 4B, Mistral 7B, and OLMo 2 7B. Supporting identity/margin, final-MLP, and crosscoder analyses use this smaller-family scope unless explicitly

marked otherwise. The Qwen2.5 32B pair is included in the main factorial and omitted from these support analyses for compute.

**Prompt supports and sampling.** All prompt supports are fixed JSONL manifests generated by `scripts/data/build_eval_dataset_v2.py`. The full manifest has 1400 records; the Core-5 headline support has 600 records. Records contain a stable `id`, `category`, `source`, raw prompt text, and task metadata where available.

**Table A.1: Prompt support composition.**

Support	Size	Composition	Paper role
Full evaluation manifest	1400 records	CONTENT-FACT 300; CONTENT-REASON 200; GOV-FORMAT 250; GOV-CONV 300; SAFETY 150; GOV-REGISTER 100; BASELINE-EASY 100	parent manifest for held-out and stress-test supports
Holdout-600	600 records	GOV-CONV 300; GOV-FORMAT 150; SAFETY 150	Core-5 headline first-divergence support
Content/reasoning-enriched stress support	5889 valid units	MMLU CONTENT-FACT; GSM8K CONTENT-REASON; smaller IFEval GOV-FORMAT slice	checks that the pattern is not confined to response-shaping/safety prompts

Exact support identifiers are: full manifest `data/eval_dataset_v2.jsonl`, headline holdout `data/eval_dataset_v2_holdout_0600_1199.jsonl`, and the content/reasoning-enriched Exp23 residual-factorial artifact listed in Appendix H.

The full manifest is intentionally mixed. CONTENT-FACT records are MMLU multiple-choice questions (Hendrycks et al., 2021); CONTENT-REASON records are GSM8K reasoning prompts (Cobbe et al., 2021); GOV-FORMAT records are IFEval prompts with explicit instruction-following/format-compliance criteria (Zhou et al., 2023); GOV-CONV combines 200 custom governance/assistant-conversation prompts, 80 MT-Bench prompts (Zheng et al., 2023), and 20 project-authored WildChat-style prompts (Zhao, W. et al., 2024); SAFETY contains 75 harmful/refusal prompts (69 AdvBench prompts from Zou, Wang, Kolter, and Fredrikson, 2023, plus 6 custom prompts in the committed manifest) and 75 safe comply prompts (`custom_safe`, XSTest-style safe prompts from Roettger et al., 2024, in the metadata). Here GOV denotes governance/assistant-behavior supports rather than a government domain: GOV-CONV is open-ended conversational governance, while GOV-FORMAT is explicit response-format compliance. GOV-REGISTER and BASELINE-EASY are custom auxiliary categories used outside the Core-5 headline support.

The holdout-600 support is the fixed slice used for the Core-5 headline factorial. It contains only governance conversation, formatting, and safety prompts: GOV-CONV/GOV-FORMAT/SAFETY = 300/150/150. The Qwen2.5 32B raw run was collected on a larger support, but the Core-5 synthesis restricts it to this same holdout mix (599 valid events because one safety prompt has no first divergence).

The content/reasoning-enriched stress support is separate from the Core-5 headline average. It was run to test whether the late-stack pattern that depends on IT upstream state survives on prompts less dominated by assistant-opening, formatting, and safety behavior. The run uses raw-shared first-divergence collection over five dense families available for that stress test (`gemma3_4b`, `llama31_8b`, `mistral_7b`, `o1mo2_7b`, `qwen3_4b`) and produces 5889 valid first-divergence units across 2983 prompt clusters with 0 invalid events. The analyzed prompt-source counts are MMLU 2837 units

over 1485 clusters, GSM8K 2087 units over 999 clusters, and IFEval 965 units over 499 clusters. This stress support is reported as a robustness check only; it is not pooled into the Core-5 headline magnitude.

For all raw-shared first-divergence and residual-state runs, PT and IT branches receive the same raw prompt text, and the runner validates identical raw prompt token IDs before comparing residual states. Starting from that shared prompt, both checkpoints are greedily decoded until the first top-1 disagreement, with a real-token mask and at most 128 generated tokens. Events are excluded if the record is malformed, no first disagreement is found within the generation budget, a required model file is missing, or the token/readout validity checks fail. Position 0 is therefore the first generated token after the full raw prompt, not a chat-template artifact. Unless otherwise stated, bootstrap intervals resample prompt clusters within family.

**Minimal reproducibility snapshot.** Revision prefixes are unique abbreviations of the pinned Hugging Face revisions listed below.

**Table A.2: Core-5 reproducibility snapshot.**

Family	PT rev.	IT rev.	Valid events	First-div.		Late stack
				position 0 / >= 3	/ >= 5	
Llama 3.1 8B	d04e592	0e9e39f	600/600	59.3% / 28.0% / 17.3%		layers 19-31
Qwen 3 4B	906bfd4	1cfa9a7	600/600	48.7% / 35.2% / 23.5%		layers 22-35
Mistral 7B	caa1feb	c170c70	597/600	30.8% / 31.3% / 20.1%		layers 19-31
OLMo 2 7B	7df9a82	470b1fb	586/600	60.1% / 27.1% / 16.0%		layers 19-31
Qwen2.5 32B	1818d35	5ede1c9	599/600	46.4% / 39.4% / 28.9%		layers 38-63

All rows use the holdout-600 support and the raw-shared first-divergence procedure above. Bootstrap unit is the prompt cluster within family.

**Pinned checkpoint identifiers.** The PDF uses short revision prefixes to keep the table readable; the supplementary manifest stores full 40-character revisions.

- Llama 3.1 8B: meta-llama/Llama-3.1-8B -> meta-llama/Llama-3.1-8B-Instruct (d04e592 -> 0e9e39f).
- Qwen 3 4B: Qwen/Qwen3-4B-Base -> Qwen/Qwen3-4B (906bfd4 -> 1cfa9a7).
- Mistral 7B: mistralai/Mistral-7B-v0.3 -> mistralai/Mistral-7B-Instruct-v0.3 (caa1feb -> c170c70).
- OLMo 2 7B: allenai/OLMo-2-1124-7B -> allenai/OLMo-2-1124-7B-Instruct (7df9a82 -> 470b1fb).
- Qwen2.5 32B: Qwen/Qwen2.5-32B -> Qwen/Qwen2.5-32B-Instruct (1818d35 -> 5ede1c9).

The Core-5 synthesis combines stored per-family prompt-bootstrap estimates for the five families in Sec. 2.1. Secondary scale conversions include the matched/portable ratio:

$$\text{matched/portable ratio} = [Y(U\_IT, L\_IT) - Y(U\_IT, L\_PT)] / [Y(U\_PT, L\_IT) - Y(U\_PT, L\_PT)].$$

This secondary scale compares the same IT late-stack replacement under the two upstream states. We also report a native-shift scale, computed inside the same 2x2:

$$\text{native PT-to-IT diagonal margin shift} = Y(U\_IT, L\_IT) - Y(U\_PT, L\_PT).$$

The reported interaction share is the interaction divided by the native diagonal margin shift. This is a scale reference, not a claim that the interaction linearly decomposes all behavioral difference.

## B Main First-Divergence Cross-Patching Audit Trail

**Claim supported.** The Core-5 first-divergence interaction is positive across families and decomposes into a portable PT-upstream component plus a larger component under IT upstream state under both common readouts.

**Primary evidence.** Core-5 common-IT/common-PT four-cell summaries, family-level interaction ranges, and the content/reasoning-enriched stress test.

**What this does not prove.** The prompt-bootstrap intervals are conditional on sampled prompts and released checkpoints; they are not population-level uncertainty over all post-training recipes.

**Where to audit.** Core synthesis artifacts, raw first-divergence mirrors, and Qwen2.5 32B support are listed in Appendix H.2.

Main Core-5 effects:

**Table B.1: Core-5 four-cell effect summary.**

Scope	PT-up late	IT-up late	Interaction	Ratio	Portable share
Core-5, common-IT	+0.759 [+0.682, +0.835]	+2.439 [+2.344, +2.533]	+1.680 [+1.604, +1.756]	3.2x	31.1%
Core-5, common-PT	+0.784 [+0.717, +0.850]	+2.488 [+2.397, +2.578]	+1.704 [+1.628, +1.780]	3.2x	31.5%

The native diagonal margin shifts are +4.991 logits under common-IT readout and +5.051 under common-PT readout; the interaction is 33.7% of that native shift in both readouts.

Core-5 family-level common-IT interactions:

**Table B.2: Family-level common-IT interactions.**

Family	Interaction	Native diagonal shift	Interaction share
Llama 3.1 8B	+1.253	+5.358	23.4%
Qwen2.5 32B	+1.302	+3.995	32.6%
Qwen 3 4B	+1.464	+3.938	37.2%
OLMo 2 7B	+1.847	+5.227	35.3%
Mistral 7B	+2.534	+6.437	39.4%

The Core-5 family interaction range is +1.253 to +2.534 logits, with median +1.464. Interaction share ranges from 23.4% to 39.4%.

The portable-share family range is similarly heterogeneous. Under common-IT readout, the PT-upstream late effect divided by the IT-upstream late effect ranges from 19.5% to 44.3%, with median 29.2%; the Core-5 family-balanced center is 31.1%. We report the family range where heterogeneity matters and use 31.1% only as a center-of-mass summary of the local token-margin contrast, not as a constant across families or as a deployment-level transfer estimate.

The Core-small label-swap null is computed from the compatibility-permutation synthesis in Appendix H.2.

On the content/reasoning-enriched stress-test support, the late-only PT-upstream term is -1.176 and the upstream x late interaction is +1.812 ([+1.721, +1.901]).

The Qwen2.5 32B scale-check artifacts include both the larger raw run and the matched-support holdout synthesis; Appendix H.2 lists both audit paths.

## C Validation Controls

**Claim supported.** The main upstream x late interaction is not made uninformative by broken hybrids, arbitrary selected-token support, first-divergence-only support, or pre-late logit commitment.

**Primary evidence.** Hybrid interpolation is smooth and positive, random local disagreements retain a reduced but same-sign interaction, native-history local disagreements remain positive, pre-divergence future-token scoring is near zero, and pre-late logit-commitment restrictions preserve the interaction.

**What this does not prove.** These controls do not make hybrid states natural deployment trajectories, nor do they estimate completion-level behavior; they show that the main artifact explanations are unlikely to account for the measurement.

**Where to audit.** Full validation artifacts and scripts are listed in Appendix H.2.

**Table C.1: Validation control summary.**

Check	Result	Takeaway
Hybrid endpoint interaction	+1.794	Constructed cells reproduce the expected endpoint effect.
PT-to-IT interpolation slope	+1.831	The effect grows smoothly along the residual-state interpolation.
Signed-permutation random/observed ratio	0.31x	Matched-magnitude random signed patches do not reproduce the effect.
Random local disagreement	+1.005 (56% of first divergence)	First divergence is high-signal, not the only same-sign support.
Native-history local disagreements	IT-history +1.51, PT-history +1.49	The interaction persists after native continuations at horizons h=4,8,16.
Pre-divergence future token pair	+0.059 (3%)	The token pair matters; arbitrary earlier prefixes do not carry the effect.

### C.1 Hybrid-State Validation

Key checks are summarized over the Core-small support families:

**Table C.2: Hybrid-state validation.**

Check	Result
Endpoint interaction, common-IT	+1.794
PT-to-IT interpolation slope	+1.831
Signed-permutation random/observed ratio	0.31x

These checks target the main off-manifold worry. A pathological hybrid artifact would more naturally appear as endpoint mismatch, non-smooth interpolation, or a matched-magnitude random intervention producing similar effects. We do not see that pattern.

### C.2 Selection and Token-Support Controls

The main-text figure and table below report Core-small family-balanced means computed from the per-family random-disagreement summaries.

**Table C.3: Selection and token-support controls.**

Condition	Interaction	Share of first divergence
True first divergence	+1.794	100%
Random local disagreement, source-balanced	+1.005	56%
Random PT-rollout disagreement	+0.836	47%
Random IT-rollout disagreement	+1.190	66%
Pre-divergence prefix, future token pair	+0.059	3%

Random local disagreements are later and more content-token-heavy than first divergences, yet their factorial interaction is smaller. The selected-support audit likewise finds that most labeled first-divergence events fall in substantive instruction, safety, formatting, response-shaping, or semantic-content categories rather than pure surface formatting. We keep the full category table in the artifact report because it is a support audit, not part of the evidence spine.

### C.3 Pre-Late Logit-Commitment Control

The support-run control restricts to events where the IT boundary readout does not yet favor  $t_{IT}$ , bins events by IT boundary margin, and fits boundary-margin controls. In all three views the interaction remains positive. This rules out the simplest “the late stack is irrelevant because the boundary already committed” reading without promoting these support-run magnitudes to Core-5 headline estimates.

### C.4 Native-History Local-Disagreement Check

This check drops the shared-history first-divergence support. For each prompt, we greedily generate a native PT or IT history, take fixed horizons  $h = 4, 8, \text{ and } 16$ , keep horizons where the two checkpoints disagree on the next token at that native prefix, and run the same four-cell late-stack factorial. The run covers the four Core-small dense families (Llama, Qwen3, Mistral, OLMo); all 3000 prompt rows are valid and diagonal no-op patch deltas are 0.0.

**Table C.4: Native-history local-disagreement check.**

Native-history support	Interaction	Events / prompt clusters	Family sign
IT history, $h=4,8,16$	+1.514 [+1.418, +1.607]	2035 / 1466	4/4
PT history mirror, $h=4,8,16$	+1.490 [+1.334, +1.646]	551 / 355	4/4

Because the PT-history mirror is also strongly positive, the claim is native-history/local-disagreement generalization rather than IT-history specificity. This does not turn the measurement into a deployment-level behavior measure; it shows that the late-stack pattern is not confined to the first shared-history disagreement.

## D Depth and Terminal Anatomy

**Claim supported.** Middle windows are relatively more candidate/identity-selective, while late and terminal windows are more margin/readout-sensitive.

**Primary evidence.** Identity-transfer and margin-support tables, terminal-depth retention, and terminal-MLP margin interaction.

**What this does not prove.** The depth windows are not modular circuits, and the boundary between “middle” and “late” is graded.

**Where to audit.** Depth-anatomy artifacts are listed in Appendix H.2.

Main depth-anatomy quantities:

**Table D.1: Depth-anatomy quantities.**

Readout	Early	Middle	Late / terminal	Interpretation
PT host: IT-token identity transfer	-	25.6%	18.8%	Middle substitutions transfer candidate identity more often.
IT host: PT-token identity transfer	-	28.2%	21.5%	Mirror direction gives the same identity pattern.
Pure IT MLP support for t_IT	-0.085	+0.136	+0.986	Native IT-token support is late- concentrated.
PT-host late MLP margin gain	-	-	+0.004	Late MLP updates alone are near zero in PT upstream state.
Source decomposition interaction	-	-	+0.360	MLP-level readout also shows context gating.

In the Core-small support set, the final-three stack retains 52% of the same-prompt full-late interaction; the final block alone retains 23%. Final-three MLP substitutions transfer IT-token identity 8.8% of the time, with final-MLP margin interaction +0.524 ([+0.491, +0.558]). The final layer alone gives final-MLP margin interaction +0.146 ([+0.128, +0.165]).

## E Sparse Final-Layer Feature Bridge

**Claim supported.** Causally ranked final-layer crosscoder features and structured boundary-state shifts carry concentrated, partial bridges for the final-layer readout interaction.

**Primary evidence.** Top-200 causal features mediate 26-48% of the final-layer interaction in three quality-gated families, matter more under IT upstream state, partially rescue the weak hybrid, and respond to earlier-layer patches. Separately, train-fit PCA components of the descendant-minus-base boundary-state shift close much of the missing margin at final-layer boundaries.

**What this does not prove.** This is not full circuit recovery, and it does not prove feature monosemanticity. The crosscoder edits are quality-gated tests on the same constructed hybrid distribution, not proof that every hybrid activation lies inside the native crosscoder training distribution. The boundary-state closure test is not recipe-unique and does not estimate completion-level behavior. OLMo is excluded from feature-level claims because its final-layer crosscoder did not pass the reconstruction gate.

**Where to audit.** Crosscoder training, mediation, gating, feature rescue, structured boundary-state closure, handoff, autointerp, and structure-readout artifacts are listed in Appendix H.2.

### E.1 Final-Layer Crosscoder Mediation and Upstream Dependence

For a feature set  $S$ , the mediation table uses the same four-cell interaction as the main cross-patching result. Let

$$I_{\text{full}} = [Y(U_{\text{IT}}, L_{\text{IT}}) - Y(U_{\text{IT}}, L_{\text{PT}})] - [Y(U_{\text{PT}}, L_{\text{IT}}) - Y(U_{\text{PT}}, L_{\text{PT}})].$$

We ablate S only in the two cells that use the IT final layers, (U\_IT,L\_IT) and (U\_PT,L\_IT), leaving the two PT-late cells unchanged, and recompute the interaction as I\_ablate(S). The reported top-200 drop is therefore:

$$\text{interaction\_drop}(S) = I_{\text{full}} - I_{\text{ablate}}(S).$$

The displayed share is  $\text{interaction\_drop}(S) / I_{\text{full}}$ , computed from the family-level mean interaction and mean drop in this mediation replay. It is not a single-cell ablation divided by a difference-in-differences. The later causal-gate audit is a separate upstream-dependence stress test and is not a replacement numerator for this mediated fraction.

In the quality column, VE is held-out variance explained by the paired crosscoder decoder branch, L0 is the mean number of active features per token, and alive is the fraction of tokens on which a feature activates. The reconstruction-quality gate requires every selected final layer to have both PT and IT held-out VE at least 0.75, mean L0 within 10% of the configured BatchTopK target, alive fraction between 0.01 and 0.20, a positive top-200 causal drop, and matched-random drop no larger than 0.05.

**Table E.1: Final-layer crosscoder mediation.**

Family and scope	Quality gate summary	Top-200 interaction drop	Drop / final-layer interaction	Matched random drop
Llama, final 3 layers	VE min 0.774; L0 64; alive max 0.096	+0.599 [+0.469, +0.733]	48%	-0.209 [-0.255, -0.165]
Mistral, final 3 layers	VE min 0.786; L0 64; alive max 0.089	+0.684 [+0.600, +0.764]	26%	-0.100 [-0.159, -0.044]
Qwen, final 2 layers	layer VE 0.957/0.960 and 0.967/0.970	+0.324	37%	-0.033

OLMo final-layer crosscoder quality did not pass this predeclared reconstruction gate, so OLMo is excluded from feature-level claims.

The artifact report includes mediation curves that sweep the number of ablated causally ranked features; the paper table below gives the corresponding top-200 and top-500 summaries. The main table reports top-200 because it is fixed across families and far from the full-dictionary reconstruction setting; the top-500 comparison checks that the effect is not a single hand-picked feature count. The top-200 set is a small causally ranked subset of the crosscoder dictionary, not a full reconstruction. Reducing 26-48% of the exposed final-layer interaction by ablating this subset is therefore a concentration result; matched-random features do not reproduce it.

**Table E.2: Top-k saturation check.**

Family	top-200 share	top-500 share	Saturation read
Llama	48%	52%	modest additional distributed mass
Mistral	26%	29%	modest additional distributed mass
Qwen	37%	38%	mostly saturated by top-200

The same feature sets show causal importance that depends on upstream state in a separate hardening audit.

For the same causally ranked final-layer features, we compare ablation effects in the (U\_IT,L\_IT) and (U\_PT,L\_IT) cells. The primary feature causal gate is:

$$\text{drop}(U_{\text{IT}}, L_{\text{IT}}) - \text{drop}(U_{\text{PT}}, L_{\text{IT}}).$$

Positive values mean the feature set matters more when the IT final layers receive IT upstream state. These gate values are not used as mediated-share numerators. They are recomputed in the Exp42 upstream-dependence audit with its own event support and direct feature-ablation protocol, so their absolute magnitudes need not equal the Table E.1 interaction drops. The paper-facing use is the sign and the matched-control comparison. At top-200 features:

**Table E.3: Upstream-dependent causal gate.**

Metric	Estimate
Separate causal feature gate, clean-family mean	+0.703
Causal gate minus matched-random features	+0.887
Causal gate minus top-active noncausal features	+1.495
Margin-weighted activation gate minus matched-random features	+0.520

Per-family gates:

**Table E.4: Per-family causal gates.**

Family	Separate causal gate	Causal minus matched random
Llama	+0.922	+1.254
Mistral	+0.816	+0.982
Qwen	+0.370	+0.426

Raw decoder-weighted activation mass is not uniformly higher under IT upstream state across families. We therefore use the finite-difference causal gate as the primary upstream-dependence result and the signed margin-weighted activation gate as supporting evidence.

**E.2 Final-Layer Feature Rescue and Earlier-to-Final-Layer Handoff**

The rescue analysis tests a partial-sufficiency version of the same feature-level story. It runs on the three clean rescue families with quality-gated final-layer crosscoders (Llama, Mistral, Qwen). OLMo is excluded because its current final-layer crosscoder does not pass the reconstruction-quality gate needed for faithful feature-space rescue edits.

The edit takes the top-200 causal final-layer feature activations from the native (U\_IT,L\_IT) pass and patches them into the (U\_PT,L\_IT) hybrid, decoded through the IT branch of the paired PT/IT crosscoder. The metric is rescued IT-token margin:

$$Y(U_{PT},L_{IT} + \text{rescued features}) - Y(U_{PT},L_{IT}).$$

These rescue rows are absolute logit gains. Rescue fractions divide the gain by the missing margin,  $Y(U_{IT},L_{IT}) - Y(U_{PT},L_{IT})$ , so they are not the same unit as the logit-gain rows.

**Table E.5: Final-layer feature rescue.**

Rescue metric, Llama/Mistral/Qwen family-balanced	Estimate	95% CI
Direct top-200 causal feature rescue	+0.494	[+0.451, +0.539]
Direct rescue fraction	8.1%	[5.5%, 10.3%]

Rescue metric, Llama/Mistral/Qwen family-balanced	Estimate	95% CI
Causal minus matched-random rescue	+0.561	[+0.510, +0.613]
Causal minus matched-random rescue fraction	10.8%	[7.6%, 13.7%]
Causal minus same-delta-random rescue	+0.471	[+0.427, +0.517]
Causal minus same-delta-random rescue fraction	8.3%	[5.7%, 10.6%]

Per-family direct rescue is Llama +0.627, Mistral +0.755, and Qwen +0.101 logits. The  $\alpha=0$  no-edit sanity check is exact ( $\max |\text{rescue\_gain}| = 0$ ). This is partial sufficiency rather than circuit recovery: the selected final-layer features recover a measurable slice of the missing margin and beat both controls, but most of the (U\_IT,L\_IT) vs. (U\_PT,L\_IT) gap remains.

The earlier-to-final-layer handoff analysis tests whether upstream computation drives the selected final-layer features, rather than merely co-occurring with them. It uses the same three quality-gated feature families and top-200 final-layer causal features. In the rescue direction, we start from the weak (U\_PT,L\_IT) hybrid and replace an upstream MLP window with IT computation before running the IT final layers. In the degrade direction, we start from native (U\_IT,L\_IT) and replace the same window with PT computation. The mediated effect is the part of the margin change that disappears when the selected final-layer features are ablated in both the base and perturbed passes. The mediated fraction is estimated separately as a prompt-level fraction with finite-denominator filtering and then family-balanced; it is not the ratio of the two aggregate means shown in the neighboring columns.

**Table E.6: Earlier-to-final-layer handoff.**

Handoff window / direction	Total margin effect	Final-layer-feature- mediated part	Mediated fraction
middle-to-final- layer rescue into (U_PT,L_IT)	+1.714 [+1.634, +1.791]	+0.132 [+0.118, +0.147]	6.5%
middle-to-final- layer degradation of (U_IT,L_IT)	+3.570 [+3.427, +3.721]	+0.527 [+0.478, +0.576]	10.8%
final-layer-entry upper-bound rescue	+5.147 [+4.936, +5.351]	+0.705 [+0.643, +0.767]	12.5%
final-layer-entry upper-bound degradation	+5.147 [+4.953, +5.358]	+0.705 [+0.644, +0.762]	12.5%

The middle-to-final-layer mediated effect beats matched-random features (+0.188 rescue; +0.655 degradation), same-delta random directions (+0.115 rescue; +0.390 degradation), and top-active noncausal features (+0.496 rescue; +0.928 degradation). The final-layer-entry rows are upper-bound sanity checks: they patch directly at the boundary into the final-layer readout, so they should be larger than earlier windows. The late-before-final-only window is weaker, especially in Qwen’s event-permutation null, so the paper-facing claim is about an earlier-to-final-layer handoff, not a late-before-final-only mechanism.

### E.3 Structured Boundary-State Closure

The feature-rescue analysis edits a selected sparse final-layer feature set and reports absolute logit gains. As a complementary check, we ask whether the missing upstream state itself has a structured low-rank form. For five Llama-3.1-8B descendants, we fit PCA components to train-split descendant-minus-base boundary-state shifts and inject held-out projections into the weak base-upstream/descendant-late hybrid. The rank-256 rows are the main structured-closure test; the full-delta rows are upper-bound sanity checks. Closure fraction is:

$$[\text{rescued margin} - \text{floor margin}] / [\text{native descendant-upstream margin} - \text{floor margin}].$$

**Table E.7: Structured boundary-state closure.**

Boundary	Train-fit PCA rank-256	Full-delta upper bound	Gaussian full	Random full	Sign-flip full
29	0.634	0.929	-0.019	-0.036	-0.816

The same-base wrong-descendant controls are nonzero in the artifact report, so we do not interpret these PCA directions as recipe-unique. The defensible claim is narrower: the missing upstream contribution at final-layer boundaries is a structured descendant-minus-base residual-state shift, not generic perturbation magnitude.

### E.4 Descriptive Autointerp and Structure-Readout Edit

Across 225 interpreted features from the clean final-layer-crosscoder families, mean validation AUROC is 0.886. We use these labels descriptively, not as causal evidence: the causal claim remains the mediation, upstream-dependence, and rescue results above. The paper-facing semantic check is the narrower `structure_readout` bucket below, where a predeclared readable subset is edited and tested against controls.

The structure-readout edit tests one readable subset from the taxonomy rather than every label bucket. The predeclared `structure_readout` bucket contains 10 causal features across the three clean crosscoder families, with labels such as paragraph breaks, list openings, answer boundaries, and field separators. Automated labels are used as audit aids in the spirit of prior neuron-explanation work (Bills et al., 2023; Huang et al., 2023), not as proof of feature monosemanticity. This is not an N=10 statistical generalization claim: the features are the predeclared edit set, while the test is whether the edited final-layer readout changes monotonically over prompts and families and beats matched controls. Editing this bucket inside the same final-layer crosscoder windows gives a monotone dose response in interaction drop; matched-random and same-delta random controls are much smaller.

**Table E.8: Structure-readout bucket edit.**

Edit strength alpha	Structure bucket	Matched random	Same-delta random
0.0	0.000	0.000	0.000
0.5	+0.039	-0.015	+0.001
1.0	+0.078	-0.028	+0.012
1.5	+0.125	-0.041	+0.020
2.0	+0.180	-0.048	+0.039

At alpha=2.0, per-family structure-bucket interaction drops are Llama +0.091, Mistral +0.339, and Qwen +0.110. Magnitudes are heterogeneous, but all three signs are positive. We use only this selective structure/readout result in the paper-facing feature-label validation. Other bucket edits were run as diagnostics but are not part of the evidence spine because their feature support is smaller or more domain-specific.

## F Recipe, Continuation, Behavior-Audit, and Released Stage-Lineage Checks

**Claim supported.** The interaction is not merely an automatic consequence of fine-tuning/continuation pretraining (CPT) or a one-token artifact, and fixed-support versions appear coherently along two released dense post-training lineages.

**Primary evidence.** On the same Llama-3.1-8B base, general-purpose instruction-following descendants show positive interaction on instruction/format supports, while OpenMath2’s math-domain late effect is already largely portable from base upstream state. Controlled same-base code and biomedical continuation fine-tunes do not reproduce the large main-support interaction despite verified domain NLL gains. A constrained continuation bridge shows the instruction-following interaction persists beyond the selected first token. A forced-token objective bridge is strongest on CONTENT-REASON exact-answer prompts; safety is smaller, format is borderline, and open-ended conversation is not objectively scored. On Base->Final support, Tulu-3 and OLMo-2 both show partial SFT presence, and the DPO/preference checkpoint expresses most of the final measured interaction.

**What this does not prove.** These are token-factorial recipe, constrained-likelihood, forced-token objective, and cumulative checkpoint comparisons, not isolated causal attributions to training algorithms, broad completion-level behavioral interaction, or natural-rollout guarantees for each recipe.

**Where to audit.** Recipe-structure, controlled-CPT, constrained-continuation, forced-token, and stage-sweep artifacts are listed in Appendix H.2.

### F.1 Same-Base Recipe Structure

The recipe-structure check compares descendants of the same Llama-3.1-8B base. On instruction/format support, general-purpose instruction-following descendants consistently depend on their own upstream state, while the OpenMath2 domain-specialized descendant does not reproduce the same interaction. A controlled continuation-training control then asks whether same-base non-instruction CPT alone is enough.

**Table F.1: Same-base recipe control.**

Same-base descendant	Support	Interaction	Native-context late effect	Portable late effect
Meta Instruct	instr./format	+1.053	+2.070	+1.018
Tulu SFT	instr./format	+0.287	+0.895	+0.608
Tulu DPO	instr./format	+1.131	+2.196	+1.065
Tulu Final	instr./format	+1.365	+2.407	+1.041
OpenMath2	instr./format	-0.358	+1.052	+1.411

The instruction-following mean interaction is +0.959 [+0.907, +1.017]; the matched instruction-following-minus-OpenMath2 contrast is +1.335 logits after controlling for prompt category, generated-position bin, and token category. On math-domain support, OpenMath2 still does not show a positive interaction (-0.154 [-0.450, +0.128]), even though both its own-context and base-upstream late effects are large (+3.275 and +3.430). The instruction-following mean on the same math-domain support is +1.670 [+1.540, +1.795]. Thus the OpenMath2 control is not merely failing because instruction/format prompts are out of domain; in these supports, the domain late effect is already largely portable from base upstream state rather than requiring the same upstream-dependent pattern. The sign-flip null for the instruction-following orientation is clean (+0.968 observed vs +0.108 null 99.9th percentile;  $p=5e-5$ ). We use this as evidence that the readout interaction depends on training recipe, not as a claim that the same token-level interaction directly predicts natural behavior for every descendant.

We also trained two LoRA continuation adapters (Hu et al., 2022) from the same pinned Llama-3.1-8B base on code and biomedical text, merged them into BF16 checkpoints, and verified domain learning before applying the same factorial. Code CPT improves held-out code NLL by 4.66%, biomed CPT improves held-out biomedical NLL by 4.81%, and both pass merge-equivalence and generation-health checks. On the main support, code CPT is essentially zero and biomed CPT is

tiny; on biomedical support, biomed CPT has a real domain-local interaction. This separates the instruction/governance-support result from generic continuation training while leaving room for domain-local upstream dependence.

**Table F.1b: Controlled non-instruction CPT controls.**

Same-base descendant	Support	Domain NLL gate		Interaction
Code CPT	main eval	+4.66%	-0.002	[-0.011,+0.006]
Biomed CPT	main eval	+4.81%	+0.018	[+0.005,+0.033]
Code CPT	code support	+4.66%	+0.027	[-0.013,+0.070]
Biomed CPT	biomed support	+4.81%	+0.283	[+0.193,+0.386]

## F.2 Constrained Continuation Bridge

The constrained continuation bridge extends the same-base token-factorial without switching to full free-running benchmarks. Its support is the full-1400 same-base recipe support, not the Core-5 holdout-600 support: the table pools one event per valid prompt-descendant pair for the four instruction-following Llama-3.1 descendants (Meta Instruct, Tulu SFT, Tulu DPO, and Tulu Final/RLVR), giving 5432 valid N=0 events. For each event, we force the descendant-preferred token, construct short native descendant and base continuations, and teacher-force those fixed candidate sequences through the same four hybrid cells. The sequence margin is the log probability of the descendant candidate minus the base candidate; N=0 recovers the one-token factorial on this support, while N>0 asks whether the interaction persists over short continuations.

Because this analysis re-scores the four cells in bf16 runtime conditions, N=0 cell values do not reproduce the Sec. 3.1 estimates bit-exactly: median maximum drift is 0.125, q99 is 0.375, and 61/13664 comparisons exceed 0.5. We therefore use aggregate horizon estimates rather than eventwise exact equality.

**Table F.2: Constrained continuation bridge.**

Instruction-following descendants, common-descendant readout	C_N interaction	Tail-only C_N	Events
N=0	+1.50 [+1.45, +1.56]	-	5432
N=1	+1.97 [+1.90, +2.04]	+0.43 [+0.39, +0.46]	4801
N=2	+1.74 [+1.66, +1.81]	+0.56 [+0.51, +0.60]	3607
N=4	+2.06 [+1.97, +2.16]	+0.89 [+0.83, +0.96]	3471
N=8	+2.71 [+2.59, +2.84]	+1.54 [+1.45, +1.64] (+0.193/token)	3422
N=8 same-forced descendant-tail control	+2.46 [+2.35, +2.59]	-	3850
N=8 shuffled descendant-tail control	+0.87 [+0.77, +0.97]	-	3523

Controls keep the interpretation local. At N=8, the same-forced-descendant-tail control is also positive (+2.46 [+2.35, +2.59]), showing that the effect persists after the forced first token; shuffled descendant tails are much smaller (+0.87 [+0.77, +0.97]), showing that coherent native descendant tails carry substantially more interaction than arbitrary descendant tails. This is constrained likelihood evidence, not a natural-rollout behavior estimate.

The horizon filter is not ignored. The N=8 row contains the 3422 events whose candidate sequences remain valid for eight tokens; on that same survivor subset, the N=0 interaction is +1.17, while the N=8 interaction is +2.71. The growth is therefore not solely a population-shift artifact from dropping shorter valid continuations.

OpenMath2 again has a different profile. On math-domain support, the common-descendant interaction is near zero at N=0 and negative at N=8 (-4.67 [-5.52, -3.82]), while common-base becomes positive by N=8 (+1.81 [+0.98, +2.61]). We use this as a readout-sensitive diagnostic for recipe structure, not as a universal sequence-level taxonomy of fine-tunes.

### F.3 Forced-Token Objective Consequence Bridge

This bridge asks whether the selected divergent token has downstream objective consequences without constructing hybrid rollouts or judging free-form completions. For each same-base first-divergence event, we force four possible first tokens – the descendant-preferred token, the base-preferred token, a rank-matched alternative, and a token-class-matched alternative – then continue with the native descendant model. Deterministic validators score either exact-answer correctness, safety/refusal compliance, or objective format criteria. The primary view is **suffix-only**: the forced token itself is excluded from scoring, so the estimate measures consequences for the continuation after the selected token.

The run contains 4127 records, 0 invalid or malformed records, 49524 branch score rows, and 29292 branch-difference rows. Validator coverage includes 200 CONTENT-REASON exact-answer prompts, 150 safety prompts, and 193/250 objectively scoreable GOV-FORMAT prompts. GOV-CONV prompts are present in the records, but the current validators do not assign them an objective primary criterion, so they are not included in the objective aggregate below.

**Table F.3: Forced-token objective consequence bridge.**

Objective category, suffix-only descendant-minus- base forced token	Delta	Events	Read
CONTENT-REASON exact answer	+0.157 [+0.120, +0.192]	980	clean strongest objective consequence bridge
SAFETY objective behavior	+0.039 [+0.014, +0.066]	747	smaller positive validator-specific effect
GOV-FORMAT objective criteria	+0.026 [-0.00004, +0.054]	714	positive but borderline under suffix-only scoring

The CONTENT-REASON result is the main use of this experiment in the paper: at first divergences with exact-answer validators, selecting the descendant-preferred token measurably improves the downstream native-descendant suffix. It is also the cleanest category for significance because the score is not a format/style preference and the forced first token is excluded from the suffix-only objective. The safety and format rows are useful checks but weaker; they show that objective scoring can detect additional positive consequences, not that the token-factorial measurement is a broad benchmark score.

### F.4 Tulu-3 Fixed-Support Stage Sweep

The primary Tulu analysis fixes the support to Base->Final first-divergence prefixes for the Llama-3.1-8B Base and Tulu-3 final checkpoint, then scores SFT, DPO, and Final on the same `t_Base/t_Final` contrast. The checkpoints share architecture; Tulu adds special tokens, so the preflight validates identical raw prompt token IDs and rejects target tokens outside the shared base vocabulary.

**Table F.4: Tulu fixed-support stage sweep.**

Tulu stage on fixed Base->Final support	Interaction score	% of Final score	Native top-1 picks $t_{\text{Final}}$
Base	0 by definition	0%	0.2%
SFT	+0.419 [+0.349, +0.491]	28.8% [25.5%, 31.8%]	56.9%
DPO	+1.216 [+1.090, +1.341]	83.6% [81.5%, 85.7%]	90.4%
Final/RLVR	+1.455 [+1.316, +1.606]	100%	99.1%

Base interaction is zero by definition because Base is the reference checkpoint; the nonzero native top-1 rate reflects rare cases where the Base native readout still selects the final-token label under the fixed token contrast.

The fixed-support label-swap null passes the same orientation test as the main factorial: the observed final interaction is +1.455, while the null 99.9th percentile is +0.296 ( $p=5e-5$ ). Native readout is nearly identical (+1.470 final interaction). Position  $\geq 3$  remains positive for all stages (+0.172, +0.770, +0.770).

Two base-anchored support checks ask whether the Base->Final support is doing the work. On Base->SFT support, the final checkpoint interaction is +1.322; on Base->DPO support, it is +1.436. Both label-swap nulls pass at  $p=5e-5$ , and both show the same qualitative pattern: SFT is real but smaller, while the DPO checkpoint reaches most of the final-support interaction.

**Table F.5: Tulu base-anchored support checks.**

Tulu support	Valid events	SFT score	DPO score	Final score
Base->Final	585/600	+0.419	+1.216	+1.455
Base->SFT	564/600	+0.401	+1.146	+1.322
Base->DPO	583/600	+0.427	+1.241	+1.436

## F.5 OLMo-2 Fixed-Support Stage Sweep

The primary fixed-support sweep fixes the support to Base->RLVR first-divergence prefixes and scores every intermediate checkpoint against the same  $t_{\text{Base}}/t_{\text{RLVR}}$  contrast. This makes SFT, DPO, and RLVR cumulative estimates comparable on the same local support. The older adjacent-pair analysis is retained only as historical motivation because each adjacent contrast uses its own first-divergence support and token labels; those adjacent estimates are useful local contrasts, but they are not additive attributions to the final Base->RLVR contrast.

**Table F.6: OLMo fixed-support stage sweep.**

Stage on fixed Base->RLVR support	Interaction score	% of Final score	Native top-1 picks $t_{\text{RLVR}}$
Base	0 by definition	0%	0.0%
SFT	+0.773 [+0.674, +0.873]	40.2% [37.6%, 42.8%]	61.0%
DPO	+1.629 [+1.473, +1.793]	84.7% [83.3%, 86.0%]	93.0%
RLVR/Instruct	+1.924 [+1.747, +2.104]	100%	99.7%

Base interaction is zero by definition because Base is the reference checkpoint.

The fixed-support label-swap null passes the same orientation test as the main factorial: the observed RLVR interaction is +1.924, while the null 99.9th percentile is +0.382 ( $p=5e-5$ ). Position  $\geq 3$  remains positive for all stages (+0.283, +0.677, +0.813). The result is a local lineage case study: in this released OLMo-2 path, the measured upstream-dependent interaction is partly present in the SFT checkpoint, largely present in the DPO checkpoint, and strongest in the final RLVR/Instruct checkpoint.

## G Architecture and MoE Scope

**Claim supported.** The current paper is a dense-family result, with architecture and MoE scope explicitly bounded.

**Primary evidence.** Core-5 covers dense transformer families plus a 32B dense scale check; MoE is artifact-only.

**What this does not prove.** The result may not transfer unchanged to MoE models, expert-routing interventions, or controlled attention-architecture comparisons.

**Where to audit.** Dense/MoE scope and artifact roots are summarized in Appendix H.

The Core-5 set covers dense transformer families only. It includes one Mistral family with an attention variant and one 32B Qwen scale check, but it is not a controlled architecture sweep. MoE generalization remains open: DeepSeek-V2-Lite is artifact-only because expert routing, expert swaps, and sparse activation patterns require additional controls beyond the dense-stack cross-patching test used here. The clean follow-up is to run the same first-divergence cross-patching analysis across multiple MoE base/instruct pairs with expert-routing controls and to separate attention-pattern effects from post-training recipe effects.

## H Reproducibility and Artifact Map

**Claim supported.** The paper can be audited from committed summary artifacts, with raw rerun scope and hardware requirements made explicit.

**Primary evidence.** CPU synthesis paths reproduce paper-facing tables/figures from committed JSON/CSV summaries; raw intervention reruns are mapped separately.

**What this does not prove.** Full raw GPU reproduction is cheap or necessary for every reviewer.

**Where to audit.** This appendix is the audit map.

We provide a CPU-only reviewer artifact bundle that regenerates all paper tables and figures from committed JSON/CSV summaries. Artifact paths below use the anonymized archive layout intended for supplementary submission. Full raw intervention reruns require multi-GPU hardware and are optional for audit; large raw mirrors, if supplied, should be provided through anonymous object-store links with the same logical names.

### H.1 Reviewer-Facing Reproduction Path

**Table H.1: Reviewer-facing reproduction levels.**

Reproduction level	What it reproduces	Hardware
CPU synthesis	Paper tables and figures from committed JSON/CSV artifacts.	CPU
Small raw rerun	One 4B/7B family first-divergence cross-patching run and analysis.	1-8 A100/H100/RTX PRO 6000 GPUs, depending on batching
Full raw rerun	Core-small dense runs plus the Qwen2.5 32B pair and feature experiments.	Multi-GPU A100/H100/RTX PRO 6000-class jobs

**Approximate compute budget.** We report GPU time as 80GB-class GPU-hours, counting one GPU used for one wall-clock hour as one GPU-hour. This is an engineering audit estimate, not a FLOP count: runs mix A100, H100, and RTX PRO 6000 96GB hardware, model-download/cache overhead, CPU synthesis, and failed or smoke-test retries. The successful paper-facing GPU runs used approximately 1.4k GPU-hours; including exploratory pilots, failed preflights, and reruns used during method development, the total project budget for this paper was approximately 2.0k GPU-hours.

**Table H.2: Approximate compute budget.**

Compute group	Included runs	Approx. GPU-hours
Core first-divergence factorial, Qwen2.5 32B pair, and content/reasoning-enriched stress support	Core-5 raw collection/synthesis, 32B holdout restriction, Exp23 stress support	300
Hybrid/selection/pre-late validation controls	off-manifold validation, random-local/pre-divergence controls, native-history local disagreements, pre-late logit-commitment checks	250
Depth, final MLP, and feature-level analyses	handoff runs, final-depth/MLP audits, crosscoder training/mediation, feature gating/rescue/handoff, structure bucket	550
Recipe, stage, continuation, and structured-state checks	Tulu/OLMo sweeps, same-base recipe controls, controlled CPT controls, constrained continuation, static-chimera/structured-rescue checks	350
CPU/API-only paper-facing analyses	table/figure synthesis and bootstrap analysis	0 local GPU
Exploratory pilots and failed/smoke reruns not used as headline evidence	early pilots, preflight failures, debugging reruns	additional ~ 600

**Model and dataset licenses.** Licenses below are the upstream Hugging Face or project-card licenses as checked on 2026-05-05; we do not redistribute model weights in the supplement. This table is documentation for reproducibility and is not legal advice.

**Table H.3: Model and dataset license documentation.**

Resource group	Paper use	Upstream license
Meta Llama 3.1 8B and Llama 3.1 8B Instruct	Core Llama PT/IT pair; Meta Instruct same-base descendant	Meta Llama 3.1 Community License (llama3.1)
Tulu-3 Llama 3.1 descendants and OpenMath2-Llama3.1-8B	same-base recipe and Tulu stage checks	Meta Llama 3.1 Community License (llama3.1)
Exp53 code and biomedical CPT controls	controlled non-instruction continuation fine-tunes on the Llama-3.1-8B base	Meta Llama 3.1 Community License for base weights; code rows filtered to permissive licenses; biomedical rows filtered to Creative Commons/CC BY/CC0 metadata
Qwen3 4B Base/Instruct and Qwen2.5 32B Base/Instruct	Core Qwen PT/IT pairs including the 32B member of Core-5	Apache-2.0
Mistral 7B v0.3 Base/Instruct	Core Mistral PT/IT pair	Apache-2.0
OLMo-2 1124 7B	Core OLMo pair and OLMo stage-lineage check	Apache-2.0
Base/SFT/DPO/Instruct	CONTENT-FACT prompts	MIT
MMLU (cais/mmlu)	CONTENT-FACT prompts	MIT
GSM8K (openai/gsm8k)	CONTENT-REASON prompts	MIT

Resource group	Paper use	Upstream license
IFEval (google/IFEval) MT-Bench prompts	GOV-FORMAT prompts GOV-CONV source slice	Apache-2.0 Apache-2.0 via FastChat/MT-Bench prompt releases
AdvBench / harmful safety prompts	harmful SAFETY source slice	MIT for wallledai/AdvBench; remaining harmful prompts are project-curated custom prompts
XSTest-style safe prompts and other custom prompts	safe SAFETY, GOV-CONV, GOV-REGISTER, BASELINE-EASY custom slices	committed manifest uses project-authored custom/custom_safe prompts released under CC BY 4.0 with the supplementary artifact; upstream XSTest prompts are CC BY 4.0
WildChat-style prompts	GOV-CONV style slice	project-authored style prompts released under CC BY 4.0; no WildChat records are redistributed

## H.2 Full Artifact Map

The submitted supplement contains the exact paths and SHA256 hashes for every included file in MANIFEST.sha256. The PDF keeps the audit map compact so the appendix remains readable.

**Table H.4: Compact artifact map.**

Claim group	Reproduction entry point	Supplement key
Core-5 four-cell result including Qwen2.5 32B	Core synthesis scripts and first-divergence collectors	core5; qwen25_32b; exp23_core5
Hybrid-state, token-selection, native-history, and pre-late controls	Validation and selection-control analyzers	validation; exp36; exp37; exp40; exp51
Depth and terminal anatomy	Handoff, terminal-depth, and terminal-MLP analyzers	depth_terminal; exp20; exp21; exp31-33
Sparse terminal feature bridge	Crosscoder mediation, gating, rescue, handoff, autointerp, and structure-readout analyses	sparse_features; exp34; exp39; exp41-44
Structured boundary-state closure	Static-chimera and structured-rescue analysis	boundary_state; exp48
Recipe and consequence bridge checks	Same-base recipe, controlled CPT control, forced-token objective bridge, continuation, Tulu, and OLMo analyzers	recipe_stage; exp35; exp46; exp47; exp49; exp52; exp53
Reviewer-facing CPU checks	Claim checker and minimal reproduction scripts	claim_checker; minimal_rerun

All full reruns use bf16 inference and deterministic greedy decoding unless a script states otherwise. The summary audit is CPU-only and reads committed JSON/CSV artifacts. Reproducing raw 4B-8B intervention records requires multiple 80GB A100/H100 jobs; reproducing Qwen2.5 32B additionally requires the multi-GPU run or the committed paper-facing synthesis artifacts.